DYNAMIC EVALUATION OF TIMBER POSTS FOR HIGHWAY GUARDRAILS

Jarvis D. Michie, Southwest Research Institute;
Charles J. Gatchell, Forest Product Marketing Laboratory; and
Theodore J. Duke, American Wood Preservers Institute

An experimental program was performed on guardrail posts to learn the more significant dynamic properties. A special pendulum impact facility was used to subject test specimens to dynamic loading that simulated a vehicle-guardrail installation collision. One hundred specimens of Douglas fir, southern pine, red oak, and red pine wood were evaluated; for comparison 6B8.5 and 3I5.7 steel members were tested. Sizes of wood posts ranged from 4 by 4 in. to 8 by 8 in. in cross section. The post specimens were rigidly secured in a base fixture, and the dynamic load was applied 24 in. above grade. Basic test data include a complete load resistance-post deflection determination for each specimen. The dynamic properties of peak resistance force, average resistance force, and fracture energy are reported for the four wood species and steel members. Test results show that, while data scatter exist within a wood species and size test group, the average values of such groups can be plotted in a manner to give meaningful trends. Peak force, average force, and fracture energy are shown to be a direct and linear function of moment of inertia.

•IN RECENT YEARS, highway engineers have had two main objectives in the design of guardrail and median barrier systems: first, to redirect errant vehicles in such a manner that the occupants survive the impact, and, second, to ensure that the redirected vehicle presents a minimum hazard to following and adjacent traffic. Analytical design of a system to perform these dynamic functions is a complex task for which no rigorous procedures are available. As a result, highway engineers have been compelled to develop effective guardrail systems by a trial-and-error procedure in which candidate systems are selected on the basis of individual judgment and intuition and then evaluated by full-scale crash testing. This method has proved to be slow and expensive.

More recently, analytical procedures have been developed that can characterize the vehicle-guardrail impact with excellent precision, provided that the dynamic properties of the system are known. Although meaningful results can be generated by these procedures, their widespread use has been curtailed due to insufficient information on the properties of barrier materials—in particular, on the dynamic properties of guardrail posts.

The objective of this program was to determine experimentally performance properties of timber posts when subjected to dynamic, horizontal forces. The testing procedure was designed to closely simulate the loading of a highway guardrail post when the guardrail installation is impacted by an errant vehicle. The scope of the program involved testing to failure of red oak, red pine, Douglas fir, and southern pine wood species in sizes ranging from 4- by 4-in. to 8- by 8-in. cross sections. For reference, two typical steel guardrail post shapes were also tested. The reference steel posts were 6B8.5 and 3I5.7 members.

Sponsored by Committee on Traffic Safety Barriers and Sign, Signal and Lighting Supports and presented at the 50th Annual Meeting.

EXPERIMENTATION PROCEDURE

The test apparatus and procedures were designed to subject specimens to a loading similar to that induced in highway guardrail posts when the guardrail system is hit by a typical passenger car. The test program was composed of four wood species and two steel post shapes. The specimens for each geometry evaluated are given in Table 1.

Facility

The Southwest Research Institute pendulum impact test facility consists of a pendulum, its operating equipment, and the test-control and data-acquisition instrumentation. An overall view of the facility is shown in Figure 1. A 4,000-lb mass is suspended in such a manner that it remains horizontal throughout the normal swing arc of a 26-ft radius.

Impact velocity is programmed by adjusting the vertical fall of the mass, and is calculated by the expression $V_I = \sqrt{2gh}$ where V_I is impact velocity in feet per second, g is acceleration due to gravity (32.2 ft/sec^2), and h is the mass drop height in feet. Impact velocities ranging from 0 to 40 feet per second (fps) are obtainable within the available 25-ft drop height. Other weights and mass geometrics can be used; however, the 4,000-lb mass is normally used because it represents the weight of a medium-size passenger car. A half section of an 8-in. diameter steel pipe, filled with concrete and rigidly attached to the mass, serves as the contact surface or "bumper".

Figure 1. Southwest Research Institute pendulum impact tester.

Test specimens are stationed at the lowest point of the pendulum arc where the kinetic energy (i.e., velocity) of the mass is maximum. The specimens are secured in a rigid fixture or they may be embedded in soil for cases in which the integral post-soil behavior is to be studied. Features of the post specimen and fixtures are shown in Figure 2. A firm elastomer cushion, inserted in the fixture at grade level, helps to distribute the resisting force of the fixture over the specimen width. Although the cushion reduces the degree of fixity, its purpose is to improve test simulation of the soil-embedded guardrail post by (a) permitting the specimen to deform laterally (i.e., Poisson effect) and (b) eliminating the chance of a sharp fixture edge cutting into the specimen.

The instrumentation consists of a velocity sensor and an accelerometer. A photocell, located immediately upstream from the specimen, is triggered by light-reflecting

TABLE 1

TEST SPECIMENS

Material	Dimensions (in. by in.)					
	4 by 4	4 by 6	6 by 6	6 by 8	8 by 8	9-in. Diameter
Douglas fir	8	8	—	8	8	—
Red oak	8	8	5	8	—	—
Red pine[a]	—	—	—	—	—	—
Southern pine	—	4	6	—	8	4
Steel 3I5.7	4					
Steel 6B8.5	4					

[a]16 round posts ranging in diameter from 6 to 9¾ in.

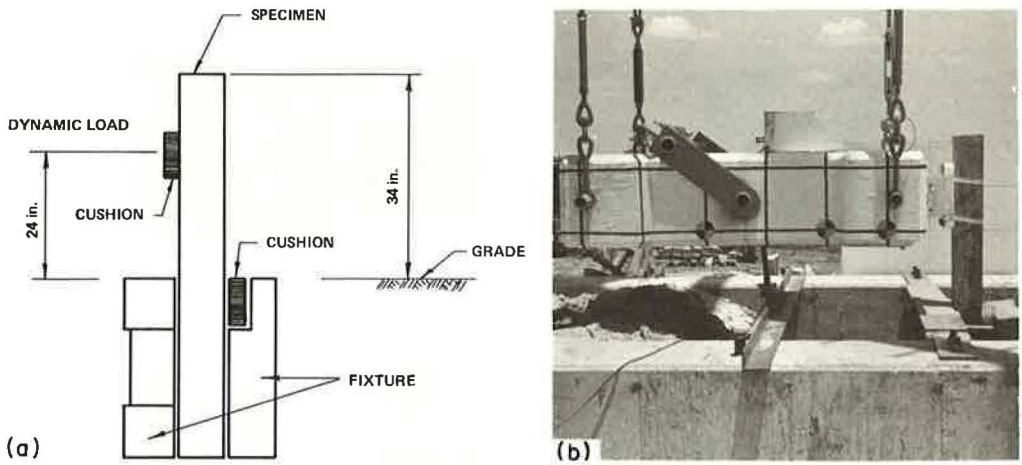

Figure 2. Features of specimen boundary conditions: (a) schematic, and (b) view prior to test.

strips attached to the lower surface of the pendulum mass. As the pendulum mass moves past the photocell, signal pulses are produced by the incrementally spaced strips. A linear strain-gage accelerometer (CEC Type No. 4-202-001, a ±25-g range), rigidly mounted to the pendulum mass at the bumper, senses the magnitudes of the pendulum mass deceleration caused by the specimen's resistance to breaking. Thus, the post's resisting force can be calculated and plotted at each instant throughout impact by multiplying mass deceleration at a particular instant by the mass weight. Signals from the velocity photocells and accelerometer are continuously recorded on a CEC VR-3300 data tape recorder. During each test, a visual record (i.e., strip chart from a Honeywell 906 C Visicorder) of the raw data is also produced to provide preliminary information and to ensure that instrumentation systems are functioning properly. A typical impact sequence is shown in Figure 3.

Procedure

After post specimens are inspected to ensure their conformance to limitations on knots, splits, and other large surface discontinuities, test numbers are assigned and the specimens' dimensions are recorded. Each specimen is inserted into the fixture with 34 in. extending above grade (Fig. 2). A firm elastomer cushion at grade level provides lateral support. Another cushion is attached to the specimen at the point of load application to attenuate the rate of force onset.

Mechanics of the test are simple. Instrumentation systems are energized and calibrated. The mass is pulled away from the impact point to an elevation calculated to provide the proper impact velocity. On signal from the test engineer, the mass is released by means of a quick-release mechanism. Instrumentation signals are continously recorded from the time of mass release, through impact, and until swing-through has been achieved. Duration of impact usually ranges from 10 to 100 msec.

Originally, an impact velocity of 30 fps was planned for all program tests. However, it became evident early in the program that only a small quantity of energy is expended in breaking the smaller posts. Consequently, the pendulum mass velocity change during impact with the smaller posts is small and difficult to measure with precision. By decreasing the impact velocity from 30 fps to 20 and 15 fps for a majority of the tests, a more discernible velocity change is effected. It was anticipated that the kinetic energy dissipated would be insensitive to this change in impact velocity. Also, the "inertia" peak in the typical force vs. time data plot is attenuated by a reduction in impact velocity. This peak, which is associated with the impulse required to accelerate the test specimen to impact velocity, is a dynamic characteristic of the specimen relating to density (i.e., mass) and is not necessarily an index of the post

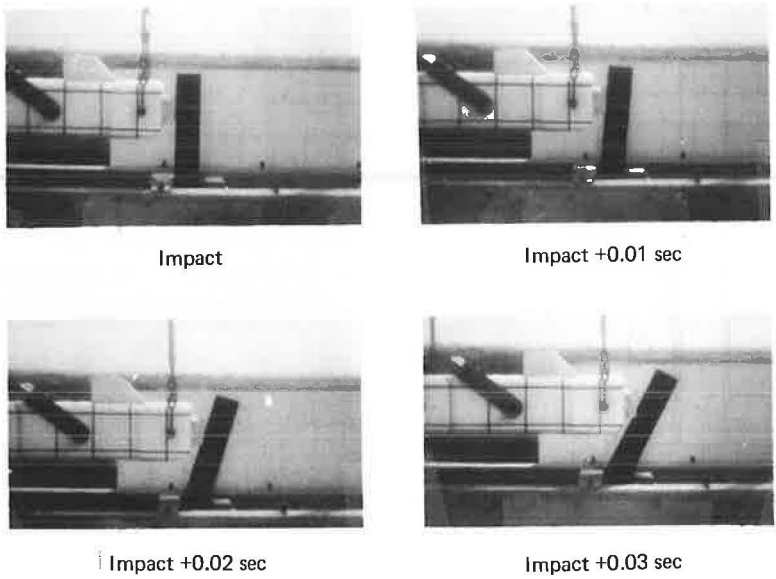

Figure 3. Pendulum specimen impact sequence.

strength. It may be of interest to note that the effect of varying the impact velocity from 30 to 15 fps is not readily apparent from the test results (i.e., post strength factors are not velocity-sensitive for these test conditions).

After the test, a section of the specimen at least 1 in. long was cut from near the failed area and weighed immediately for determination of specific gravity and moisture content. Moisture content and dry specific gravity of Douglas fir, red oak, and red pine specimens were determined by Forest Product Marketing Laboratory personnel. Although the southern pine posts were creosote-treated, the American Wood Preservers Bureau, Inc., determined the moisture content and dry specific gravity from samples taken from the failed post specimens.

FINDINGS

The types of experimental data acquired in the program, selected for the purpose of defining the post failure characteristics, were (a) peak force Fp, (b) average force F, and (c) fracture energy FE. These characteristics greatly influence the dynamic behavior of a highway guardrail installation when impacted by a fast-moving vehicle. Peak force defines the breakaway value for posts in a "weak-post" guardrail system; it also provides an input for predicting peak declerations that are induced in a vehicle during redirection. Average force is an idealized value used in the theoretical analysis of the interaction between the vehicle and the guardrail. Fracture energy of guardrail posts, in addition to other guardrail performance characteristics, is directly related to the vehicle kinetic energy dissipated during impact. These properties are shown in Figures 4 and 5 for typical timber and steel posts respectively; sample data-reduction calculations are given in the Appendix.

Findings from the experimental program are given in Tables 2, 3, 4, and 5 for red oak, red pine, southern pine, and Douglas fir timber species respectively. Data from dynamic tests performed on typical steel guardrail posts are given in Table 6 for reference.

Variation of the peak resistance force is shown in Figure 6 for Douglas fir posts. The average of data from each post size is indicated by a darkened symbol; a straight

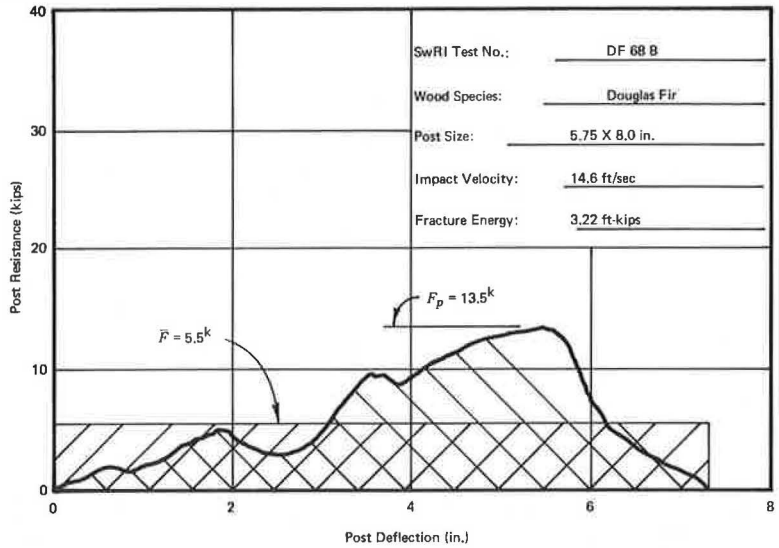

Figure 4. Typical dynamic force-deflection plot of timber specimen.

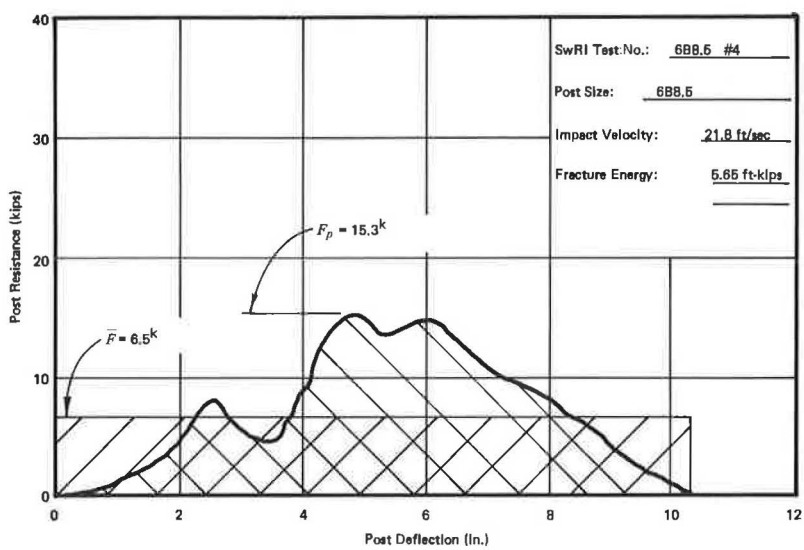

Figure 5. Typical dynamic force-deflection plot of steel specimen.

line is extended through these points. It is to be noted that the extended curve does not intersect the zero ordinate point. This anomaly may be attributed to inertia effects of the post.

Other plots of the test data are shown in Figures 7, 8, 9, and 10. The points represent the average value for the particular post specimen geometry for red oak, southern pine, and Douglas fir. For red pine, however, the specimen sizes were random, and a straight curve was statistically fitted to the data points.

TABLE 2

SUMMARY OF TEST RESULTS OF RED OAK POSTS

Specimen No.	Width (W, in.)	Depth (D, in.)	Area (A, $in.^2$)	Moment of Inertia (I, $in.^4$)	Section Modulus (S, $in.^3$)	Moisture Content (C, percent)	Specific Gravity	Impact Velocity (V_I, fps)	Impact Duration (t, msec)	Impulse (MV, lb-sec)	Fracture Energy (FE, ft-kips)	Peak Force (F_p, kips)	Average Force ($\bar{F}$, kips)
RO 44													
A	3.80	4.00	15.2	20.2	10.1	16.1	0.65	14.8	58	128	1.78	4.8	2.2
B	3.80	4.10	15.6	21.7	10.6	17.8	0.71	15.0	74	243	3.48	5.8	3.3
C	3.90	4.20	16.4	24.1	11.5	19.2	0.68	14.4	54	183	2.55	7.1	3.4
D	3.80	4.20	15.9	23.5	11.2	15.7	0.66	14.7	56	182	2.60	6.4	3.2
E	4.00	4.25	17.0	25.5	12.0	14.5	0.65	14.8	60	149	2.11	5.7	2.5
F	3.75	3.80	14.2	17.1	9.0	16.1	0.72	14.9	51	121	1.79	5.5	2.4
G	3.80	4.00	15.2	20.2	10.1	16.4	0.70	15.7	56	134	2.07	5.2	2.4
H	3.80	4.00	15.2	20.2	10.1	13.9	0.71	14.8	50	79	1.08	3.3	1.6
Average			15.59	21.56	10.58	16.21	0.685	14.89	57.4	152.4	2.182	5.5	2.62
RO 46													
A	3.90	6.00	23.4	70.2	23.4	18.3	0.58	15.0	52	231	3.16	8.4	4.4
B	4.00	6.20	24.8	79.4	25.6	18.0	0.68	14.9	59	361	4.84	11.5	6.1
C	4.00	6.00	24.0	72.0	24.0	15.1	0.74	14.9	44	278	3.77	8.7	6.3
D	4.00	6.20	24.8	79.4	25.6	16.2	0.70	15.3	48	322	4.52	10.2	6.7
E	3.80	5.90	22.4	64.9	22.0	16.4	0.75	15.5	56	326	4.58	14.1	5.8
F	4.00	6.10	24.4	75.6	24.8	15.8	0.74	15.2	53	267	3.69	11.1	5.0
G	4.00	5.90	23.6	68.7	23.3	13.3	0.75	15.7	59	348	4.98	12.3	5.9
H	3.90	5.75	22.4	61.8	21.5	15.6	0.77	15.2	50	205	2.86	11.1	4.1
Average			23.72	71.50	23.78	16.09	0.714	15.21	52.6	292.2	4.050	10.9	5.54
RO 66													
A	5.80	6.00	34.8	104	34.8	17.2	0.68	14.6	63	584	7.16	17.5	9.3
B	6.00	6.25	37.5	122	39.1	19.4	0.61	14.5	52	128	1.74	6.5	2.5
D	5.75	5.75	33.1	91	31.7	19.6	0.65	14.5	50	233	3.20	10.9	4.7
E	6.00	6.10	36.6	114	37.2	18.8	0.72	14.4	48	214	2.86	10.3	4.4
F	5.80	6.00	34.8	104	34.8	18.2	0.68	14.5	44	203	2.72	10.9	4.6
Average			35.36	107.0	35.5	18.52	0.672	14.50	51.4	272.4	3.536	11.6	5.10
RO 68													
A	5.75	8.17	46.9	261	64.0	21.6	0.68	29.6	27	202	5.73	20.4	7.5
B	5.67	7.75	43.9	220	56.8	21.4	0.62	30.1	42	280	7.92	19.0	6.7
C	6.00	8.00	48.0	256	64.0	23.6	0.68	29.9	35	335	9.58	25.9	9.6
D	6.00	8.25	49.5	281	68.1	18.7	0.67	29.8	27	209	6.11	21.4	7.7
E	5.87	7.87	46.2	238	60.6	18.1	0.64	29.2	29	230	6.32	19.2	7.9
F	5.87	8.00	46.9	250	62.6	18.6	0.67	29.7	37	333	9.51	24.8	9.0
G	6.17	7.87	48.6	251	63.7	19.2	0.75	29.7	35	330	9.17	27.2	9.4
H	5.75	7.75	44.6	223	57.6	18.7	0.70	29.6	31	172	5.03	18.2	5.5
Average			46.82	247.5	62.18	19.99	0.676	29.70	32.9	261.4	7.421	22.0	7.91

TABLE 3

SUMMARY OF TEST RESULTS OF RED PINE POSTS

Specimen No.	Diameter (d, in.)	Moment of Inertia (I, $in.^4$)	Moisture Content (C, percent)	Specific Gravity	Impact Velocity (V_I, fps)	Impact Duration (t, msec)	Impulse (MV, lb-sec)	Fracture Energy (FE, ft-kips)[a]	Peak Force (F_p, kips)[b]	Average Force ($\bar{F}$, kips)[c]
A1	6.10	68.0	13	0.34	15.1	38	60.7	0.92	4.1	2.2
A5	6.50	87.6	16	0.32	15.1	48	142.5	1.99	7.9	3.9
A4	6.60	93.2	17	0.38	15.1	42	81.9	1.28	5.7	2.8
A2	6.75	101.9	16	0.37	15.1	50	136.0	1.99	8.0	3.8
A3	7.25	135.7	22	0.34	15.1	54	253.0	3.50	12.0	6.5
A9	8.60	268.6	18	0.36	15.1	52	326.0	4.45	16.0	9.1
A8	9.10	336.7	19	0.35	15.1	62	417.0	5.66	17.1	10.3
A7	9.30	367.3	23	0.39	15.1	63	611.0	7.65	21.4	9.8
B4	6.50	87.6	14	0.33	15.1	48	131.5	1.81	8.1	3.6
B7	7.00	117.9	15	0.36	15.1	56	250.5	3.50	11.1	6.3
B3	7.00	117.9	14	0.33	15.1	47	122.8	1.81	6.5	2.7
B10	7.25	135.7	15	0.36	15.1	51	145.0	2.16	7.4	2.9
B6	7.75	177.1	17	0.38	15.1	66	491.0	6.50	16.8	11.7
B8	8.15	216.6	17	0.33	15.1	54	285.5	3.99	13.2	7.6
B9	8.50	263.3	18	0.37	15.1	90	930.0	10.57	21.3	20.5
B5	9.75	443.7	17	0.37	15.1	59	467.0	6.23	19.8	12.4

[a]Statistical curve fit to data: FE = 0.73 + 0.017 I. [b]Statistical curve fit to data: F_p = 3.96 + 0.044 I. [c]Statistical curve fit to data: $\bar{F}$ = 1.56 + 0.030 I.

TABLE 4

SUMMARY OF TEST RESULTS OF SOUTHERN PINE POSTS

Specimen No.	Width (W, in.)	Depth (D, in.)	Area (A, $in.^2$)	Moment of Inertia (I, $in.^4$)	Section Modulus (S, $in.^3$)	Moisture Content (C, percent)	Specific Gravity	Impact Velocity (V_I, fps)	Impact Duration (t, msec)	Impulse (MV, lb-sec)	Fracture Energy (FE, ft-kips)	Peak Force (F_p, kips)	Average Force ($\overline{F}$, kips)
SP 46													
A	3.88	6.00	23.3	65.4	21.8	12.4	0.46	15.4	53	209	3.07	8.9	3.9
B	3.88	6.00	23.3	65.4	21.8	11.3	0.50	14.8	38	133	1.94	7.9	3.5
C	3.88	6.00	23.3	65.4	21.8	10.0	0.46	15.2	38	141	2.00	7.6	3.7
D	3.88	6.00	23.3	65.4	21.8	11.5	0.50	15.3	50	166	2.37	8.5	3.3
Average			23.30	65.40	21.80	11.30	0.480	15.2	44.8	162.2	2.345	8.2	3.60
SP 66													
A	6.00	6.12	36.7	115	37.5	11.6	0.46	15.0	47	126	1.80	7.7	2.7
B	5.75	6.06	34.8	107	35.2	11.4	0.41	15.2	38	103	1.46	7.8	2.7
C	6.00	6.00	36.0	108	36.0	10.8	0.52	15.1	58	309	4.30	12.0	5.3
D	6.00	6.12	36.7	115	37.5	12.3	0.62	15.1	67	359	4.92	14.3	5.4
E	6.00	6.00	36.0	108	36.0	10.9	0.47	15.1	52	183	2.67	9.3	3.5
F	6.00	6.00	36.0	108	36.0	11.3	0.47	15.1	41	118	1.64	8.9	2.9
Average			36.03	110.2	36.37	11.38	0.491	15.10	50.5	199.7	2.798	10.0	3.75
SP 88													
A	7.88	8.38	66.0	386	92.2	14.0	0.53	19.9	55	637	11.7	22.0	11.6
B	8.25	8.38	69.1	405	96.6	17.7	0.51	29.8	68	637	17.3	24.3	9.4
C	8.06	8.12	65.4	360	88.6	13.1	0.53	29.4	43	506	13.9	25.9	11.8
D	8.06	8.50	68.5	413	97.1	13.3	0.50	27.6	32	233	6.3	29.4	7.3
E	8.00	8.12	64.9	357	87.9	10.7	0.56	27.6	43	470	12.1	25.2	10.9
F	8.12	8.38	68.0	398	95.0	11.2	0.46	29.6	43	452	12.4	28.4	10.5
G	7.94	8.31	65.9	380	91.4	15.1	0.54	29.2	40	366	9.9	28.0	9.2
H	8.12	8.25	66.9	380	92.1	12.8	0.58	27.6	43	424	10.9	25.4	9.9
Average			66.84	384.9	92.61	13.49	0.526	27.59	45.9	465.6	11.81	26.1	10.08
AP 9R													
A	8.38		55.1	242	57.8	9.5	0.53	20.9	34	209	4.24	14.4	6.1
B	8.75		60.1	288	65.8	12.4	0.63	20.2	44	373	6.97	20.8	8.5
C	8.00		50.2	201	50.3	11.2	0.52	20.1	43	313	5.85	17.3	7.3
D	8.38		55.1	242	57.8	11.1	0.52	20.2	35	243	4.77	15.6	6.9
Average			55.12	243.2	57.9	11.05	0.550	20.35	39.0	284.5	5.458	16.8	7.20

Note: Post specimens were creosote-treated. Specific gravity and moisture content were determined by the American Wood Preservers Bureau, Inc.

TABLE 5

SUMMARY OF TEST RESULTS OF DOUGLAS FIR POSTS

Specimen No.	Width (W, in.)	Depth (D, in.)	Area (A, $in.^2$)	Moment of Inertia (I, $in.^4$)	Section Modulus (S, $in.^3$)	Moisture Content (C, percent)	Specific Gravity	Impact Velocity (V_I, fps)	Impact Duration (t, msec)	Impulse (MV, lb-sec)	Fracture Energy (FE, ft-kips)	Peak Force (F_p, kips)	Average Force ($\overline{F}$, kips)
DF 44													
A	3.88	3.88	15.0	18.8	9.7	13.0	0.50	14.8	44	63	0.90	3.7	1.4
B	3.94	4.00	15.8	21.0	10.5	14.4	0.45	15.0	44	84	1.27	4.7	1.9
C	3.88	4.12	15.9	22.7	11.0	12.7	0.46	14.9	40	82	1.27	4.7	2.0
D	4.12	4.12	16.9	23.9	11.6	13.6	0.49	15.0	36	51	0.73	3.3	1.4
E	3.88	4.06	15.8	21.5	10.6	14.5	0.50	14.8	42	78	1.08	4.4	1.8
F	3.88	4.00	15.5	20.6	10.3	14.1	0.57	15.2	53	122	1.83	5.5	2.3
G	3.75	4.12	15.4	21.8	10.6	13.8	0.43	14.7	31	35	0.54	2.9	1.1
H	3.94	4.12	16.2	22.9	11.1	14.0	0.52	14.9	44	102	1.44	5.6	2.3
Average			15.81	21.65	10.68	13.76	0.490	14.91	41.8	77.1	1.132	4.35	1.78
DF 46													
A	4.00	6.00	24.0	72.0	24.0	15.0	0.48	15.0	36	159	2.32	10.0	4.4
B	4.12	6.00	24.7	74.1	24.7	13.0	0.50	14.8	43	182	2.61	10.5	4.2
C	3.88	6.00	23.3	69.9	23.3	17.2	0.47	14.9	48	112	1.61	6.5	2.3
D	4.25	6.00	25.5	76.5	25.5	15.8	0.44	15.0	49	137	1.98	7.4	2.8
E	4.12	6.12	25.2	78.6	25.7	15.6	0.47	15.1	50	174	2.50	7.5	3.5
F	4.25	5.88	24.9	72.0	24.5	13.8	0.44	15.0	47	97	1.45	5.9	2.1
G	4.00	6.00	24.0	72.0	24.0	15.5	0.44	14.8	46	98	1.43	5.9	2.1
H	4.00	6.00	24.0	72.0	24.0	14.7	0.46	14.8	35	90	1.25	6.8	2.6
Average			24.45	73.39	24.46	15.08	0.462	14.92	44.2	131.1	1.894	7.56	3.00
DF 68													
A	6.00	8.00	48.0	256	64.0	14.6	0.56	14.5	55	360	4.70	17.9	6.5
B	5.75	8.00	46.0	245	61.3	14.0	0.47	14.6	42	233	3.22	13.5	5.5
C	5.75	8.00	46.0	245	61.3	13.6	0.49	14.9	50	247	3.45	15.5	4.9
D	6.00	7.75	46.5	233	60.1	14.3	0.46	14.6	54	430	5.59	18.2	8.0
E	5.80	7.75	44.9	225	58.1	16.0	0.60	14.6	45	202	2.74	12.3	4.5
F	5.75	7.80	44.8	227	58.3	16.8	0.63	14.6	67	715	8.43	21.5	10.7
G	5.80	7.75	44.9	233	60.1	16.1	0.49	14.6	64	622	7.52	18.0	9.7
H	5.80	8.00	46.4	248	61.9	14.8	0.58	14.7	48	235	3.25	13.3	4.9
Average			45.94	239.0	60.64	15.02	0.535	14.64	53.1	380.5	4.862	16.28	6.84
DF 88													
A	7.60	8.00	60.8	324	81.1	14.2	0.43	15.0	61	596	7.52	22.1	9.8
B	7.60	7.88	59.9	310	78.6	14.8	0.45	14.7	77	531	6.70	16.9	6.9
C	7.75	8.00	62.0	331	82.7	14.5	0.47	14.9	63	596	7.45	21.5	9.5
D	7.60	7.88	59.9	310	78.6	14.1	0.46	14.7	67	483	6.18	17.5	7.2
E	7.60	7.88	59.9	310	78.6	15.9	0.51	15.0	58	537	6.86	20.9	9.2
F	7.60	7.75	58.9	295	76.1	16.1	0.51	14.8	63	664	8.00	23.0	10.5
G	7.75	7.75	60.1	301	77.6	14.6	0.53	14.8	65	689	8.23	22.1	10.6
H	7.60	7.88	59.9	310	78.6	15.1	0.45	14.9	63	561	7.07	19.0	8.9
Average			60.18	311.4	78.99	14.91	0.477	14.85	64.6	582.1	7.251	20.38	9.08

TABLE 6

TEST RESULTS FROM TYPICAL STEEL GUARDRAIL POSTS

Specimen No.	Section Modulus (Sx, in.^{3})	Section Modulus (Sy, in.^{3})	Impact Velocity (V_I, fps)	Impulse (MV, lb-sec)	Fracture Energy (FE, ft-kips)	Impact Duration (t, msec)	Peak Force (F_p, kips)	Average Force ($\bar{F}$, kips)
3I5.7								
1	1.7	0.40	14.8	248	3.43	74	4.9	3.4
2	1.7	0.40	14.7	264	3.56	75	5.0	3.5
3	1.7	0.40	20.8	152	3.01	53	5.5	2.9
4	1.7	0.40	14.9	336	4.55	74	6.5	4.5
Average			16.3	333	3.635	69.0	5.5	3.58
6B8.5								
1	5.07	0.96	19.7	258	4.86	37	14.3	7.0
2	5.07	0.96	14.6	506	6.40	61	15.5	8.3
3	5.07	0.96	19.8	400	7.23	50	16.0	8.0
4	5.07	0.96	21.8	273	5.65	42	15.3	6.5
Average			19.0	359	6.035	48	15.3	7.4

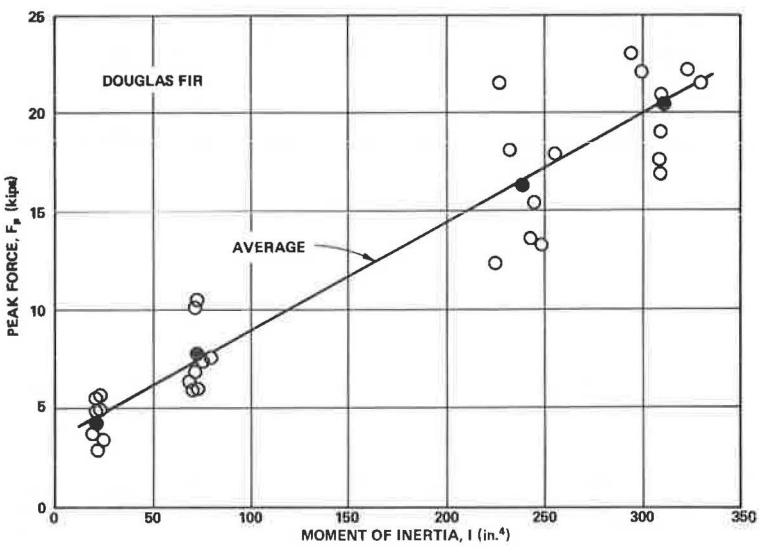

Figure 6. Variation of Douglas fir peak force with moment of inertia.

Peak resistance force plotted against moment of inertia is shown in Figure 7. Each point is the average of the four to eight tests conducted on the various sizes and wood species. With the exception of the 4- by 6-in. red oak group and the 8- by 8-in. southern pine group, the points fall quite near their respective straight lines. Douglas fir and southern pine exhibit approximately the same strength property, whereas red oak is the highest strength species and red pine the lowest strength species.

In Figure 8, average post resistance is plotted against moment of inertia. As expected, the resistance increases with moment of inertia for all species. The curves are approximately parallel with the red pine and red oak materials indicating the highest strength; the southern pine and Douglas fir curves almost coincide. It is to be noted that the shape of the post (i.e., round or rectangular) appears to have modest effect on the curves as evidenced by the 9-in. diameter southern pine specimen group point that falls on the basic curve. Clear round wood is normally 18 percent stronger in static flexure than clear rectangular wood. One point on the red oak appeared to be high and was neglected.

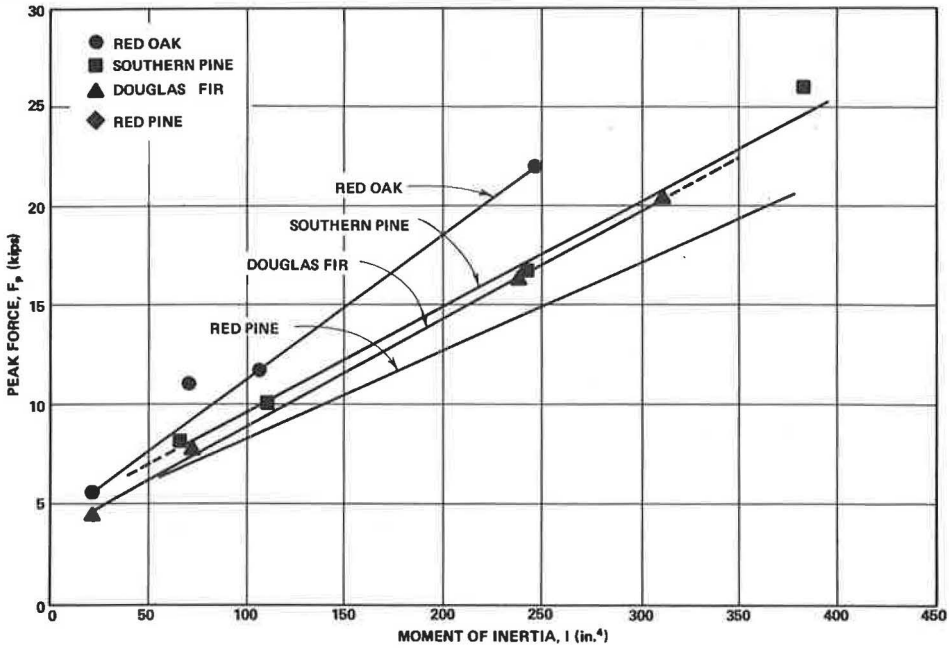

Figure 7. Variation of peak force with moment of inertia.

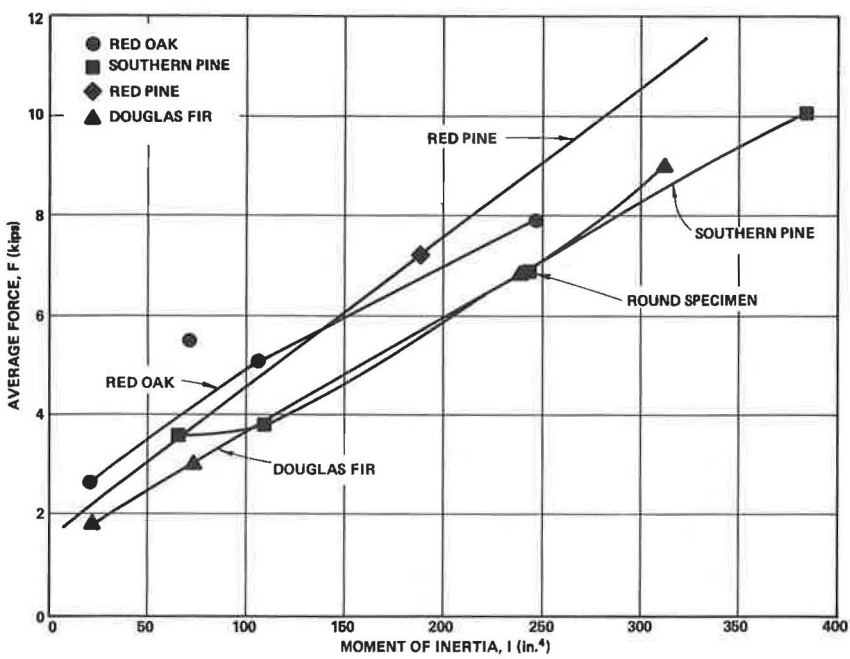

Figure 8. Variation of average force with moment of inertia.

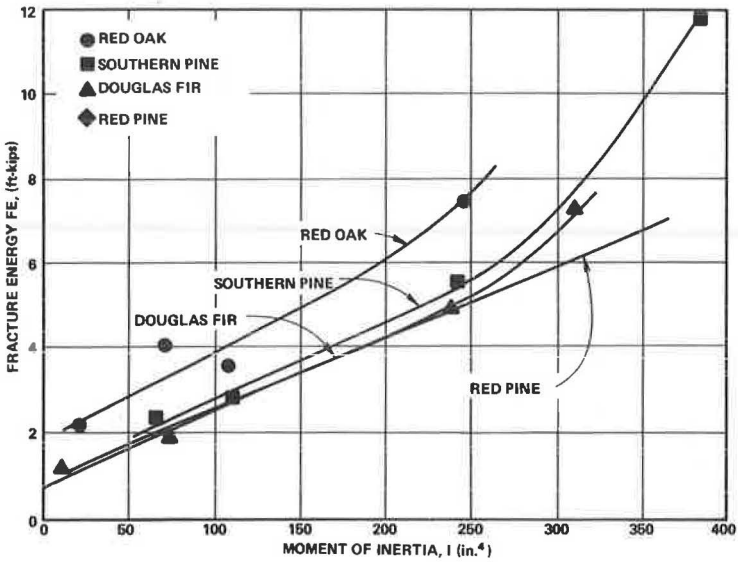

Figure 9. Variation of fraction energy with moment of inertia.

Fracture energy is plotted against moment of inertia for the four timber species in Figure 9. Red oak species possess the highest fracture energy for a given moment of inertia. The fracture energy of the other species is approximately the same. Below a moment of inertia I of 200 in.^{4}, the curves appear to be nearly linear. Above an I of

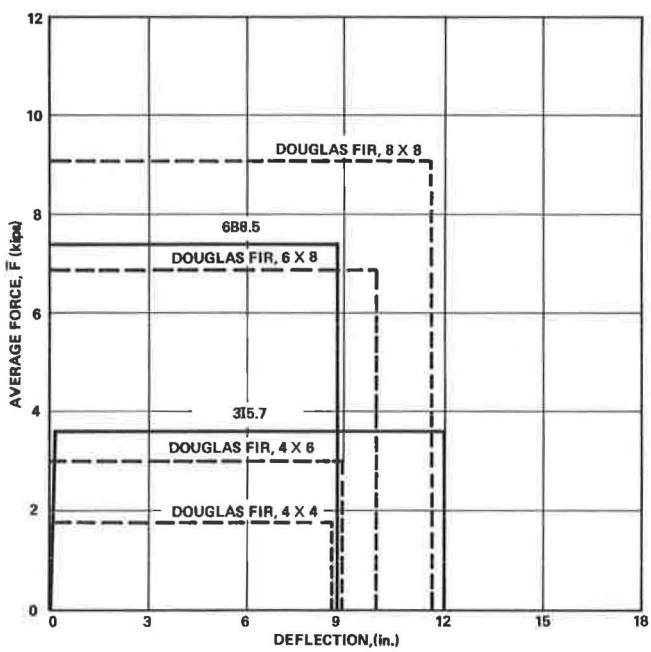

Figure 10. Average force versus deflection for typical guardrail posts.

250 in.^{4}, fracture energy indicates a tendency to increase at a more pronounced rate, particularly for Douglas fir and southern pine. It is to be noted that the shape of the southern pine specimens appears to have negligible effect on fracture energy as the round specimen group points fall on the curve connecting the rectangular-shaped specimen groups.

In Figure 10, average force is plotted against post deflection and displayed for some typical guardrail post specimens. Plots of Douglas fir specimens (4 by 4 in., 4 by 6 in., 6 by 8 in., and 8 by 8 in.) are shown with those of 6B8.5 and 315.7 steel members. In all tests, the specimens were rigidly fixed. The timber specimens fractured at the cantilever point, while the steel members twisted and bent about their weak axis. It is to be noted that the Douglas fir specimens of 6 by 8 in. and 4 by 6 in. are comparable to the 6B8.5 and 315.7 steel specimens respectively.

DISCUSSION OF FINDINGS

Several points from the program findings seem worthy of discussion and emphasis.

Test Procedure

For this program, the specimens were rigidly secured in a base fixture and then impacted with a mass possessing sufficient kinetic energy to break the specimen. Except for the so-called weak-post guardrail systems (1), guardrail posts seldom break under vehicle impact but, instead, deflect in the soil. As shown in Figure 11, in case I, the post is sufficiently embedded in the soil to develop the post strength, and it breaks prior to significant soil deformation. Cases II and III demonstrate the strong-post system in which soil failure occurs at a force on the post that is less than the post's breaking strength. Because the purpose of the program was to generate guardrail post properties and not the more complex post-soil composite properties, the soil-embedment effect was eliminated by securing the specimens in a rigid fixture.

Test Data Variation

Although there is a variation in the data of an individual specimen from its species and size group average, the average values of peak force, average force, and fracture

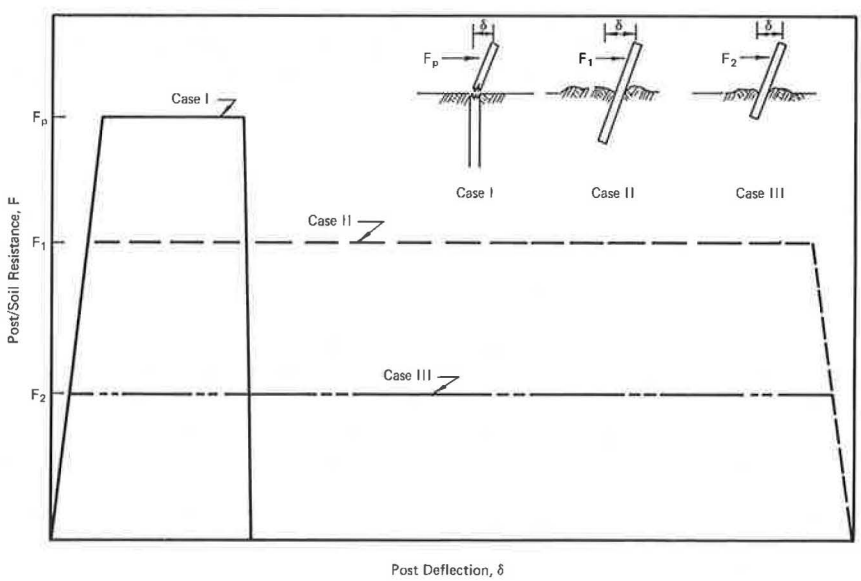

Figure 11. Idealized post-soil reactions.

energy, plotted as a function of moment of inertia, fall on or near a linear curve. This would suggest that the variation within a species and size test group has a normal distribution. On examination of the failed specimens, the variation can generally be attributed to any of several specimen imperfections such as knots, checks, shakes, worm holes, and rot located in the failure zone. Also, a portion of the data scatter is attributed to variation of ring density and specific gravity. Effects of moisture content (i.e., within normal service range) and preservative treatment on the dynamic properties of guardrail post are unknown but are surmised to be small.

Dynamic Properties

One of the three most important post dynamic properties is considered to be peak (or breaking) force. Peak force is a critical factor in the design of weak-post guardrail systems. If the post breaking force is too large, the impacting vehicle will snag on the post and spin out. Hence, higher strength is not necessarily a prerequisite of post materials for a guardrail system. On the contrary, it is suspected that the lower strength wood species may exhibit superior performance in the weak-post systems. On the other hand, if the breaking force is too small, the entire guardrail installation will collapse at initial vehicle impact. In the strong-post systems, it is necessary to provide a post strength slightly in excess of the soil resistance force (F_1 or F_2 in cases II and III respectively, Fig. 11).

The magnitude of dynamic peak force, average force, and fracture energy is a function of (a) specimen geometry and (b) wood species. As shown in Figures 7, 8, and 9, these properties vary directly with moment of inertia. (These properties also vary directly with the section area and section modulus, but the curves are nonlinear.) Specimen sectional shape does not appear to be a critical factor as square, rectangular, and round specimen data can be displayed on the same curve (Figs. 7, 8, and 9). This suggests that the engineer can use sawed or round material and expect equal performance for equal moments of inertia.

Concerning wood species, red oak, in general, exhibited the highest dynamic property values followed by Douglas fir and southern pine and then red pine. For the average force property, the red pine values were comparable to those of the red oak species. Ring density and specific gravity, possible subgroup characteristics of each wood species, appear, as one might expect, to have a meaningful influence on the properties. However, no definite conclusion on the magnitude of this effect can be deduced from the test results. Moisture content and preservative treatment also may affect dynamic properties, but results from static tests by others suggest these effects would be small. The presence of a significant degree of imperfections such as knots, checks, shakes, holes, and rot in the failure zone could significantly reduce the dynamic properties.

Application of Results

Several potential uses are suggested for the data and findings developed in the program:

1. Alternate materials may be specified for guardrail posts. By selecting a proper sectional area, the posts of alternate material will develop dynamic characteristics equivalent to those of the standard posts.
2. Dimensional tolerances for posts can be established on the basis of design performance. For instance, if a post is being selected to break within a certain dynamic force range, then the post dimensions can be established with tolerances consistent with the force range. It is to be noted that tolerances on section depth may be more critical than section width in cases where moment of inertia is a design factor.
3. Initial design of posts for new guardrail systems can be based on the experimental data.
4. The findings can be utilized in various mathematical models of a vehicle-barrier collision to improve correlation between the theoretical and physical events.
5. The findings may serve as a base line for exploring new and improved methods to convert existing strong-post systems and pole designs to breakaway designs.

REFERENCE

1. Michie, J. D., and Calcote, L. R. Location, Selection, and Maintenance of Highway Guardrails and Median Barriers. NCHRP Rept. 54, 1968.

Appendix

SAMPLE CALCULATIONS

The following calulations are used in scaling, converting, and processing experimental data from the pendulum impact facility. The basic data consist of a continuous recording of accelerometer output during specimen impact.

1. Determine acceleration magnitude of pendulum mass at time t

$$A_t = \left(\frac{d_t}{d_c}\right) A_c \tag{1}$$

where d_c is the Visicorder trace deflection (in.) resulting from the reference calibration signal corresponding to A_c acceleration (g), and d_t is the Visicorder trace deflection (in.) at any time t during test.

Example: For case where d_c, A_c, and d_t are 2.98 in., 5.2 g, and 0.75 in. respectively, then

$$A_t = \left(\frac{0.75}{2.98}\right)(5.2) = 1.31 \text{ g}$$

2. Determine magnitude of force acting on pendulum mass at time t (note that this is equal to but in the opposite direction of the force acting on the post)

$$F_t = ma_t \tag{2}$$

where m is pendulum mass (lb-sec^2/ft) and a_t (ft/sec^2) is acceleration (or deceleration) of mass.

Example: For case where pendulum weighs 4,000 lb and a_t is 1.31 g,

$$F_t = \left(\frac{4{,}000}{g}\right)(1.31 \text{ g}) = 5{,}240 \text{ lb}$$

3. Determine velocity of pendulum mass after impact. By Newton's second law of motion, the linear impulse is equal to the change in linear momentum of the pendulum mass

$$\int_{t_o}^{t_f} F_{x_t} dt = m(v_f - v_o) \tag{3}$$

where F_{x_t} is the resultant force acting on the pendulum mass in the x-direction at time t, m is the pendulum mass, and v_o and v_f are the initial and final velocities of the mass in the x-direction. A typical force-time curve is shown in Figure 12. (By definition linear impulse is equal to the area under the curve.)

Example: If the time scale in Figure 12 is 20 msec/in. and the force scale is 20,800 lb/in., then 1.0 sq in. of area represents a linear impulse of 0.020 x 20,800 or 416

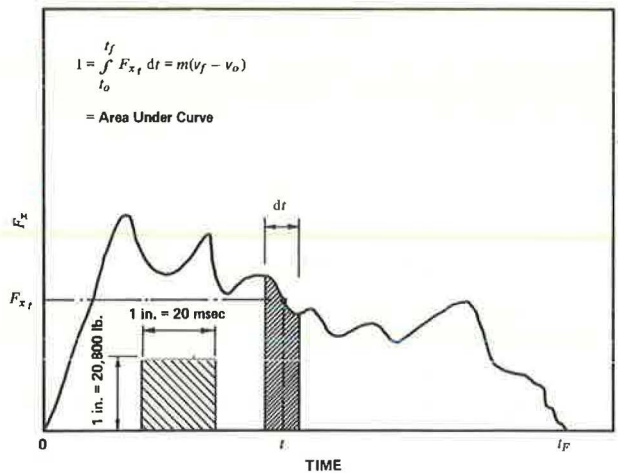

Figure 12. Pendulum mass linear impulse determination.

lb-sec/in.^{2}. If the area under the curve is determined to be 6.50 sq in., initial velocity of the mass is 30.3 fps, and the mass weighs 4,000 lb, then the final velocity can be calculated as

$$\int_{t_o}^{t_f} F_{x_t} dt = (\text{area})(K) = m(v_f - v_o)$$

$$-(6.50)(416) = \frac{4{,}000}{32.2}(v_f - 30.3)$$

$$v_f = (30.3 - 21.8) = 8.5 \text{ fps}$$

4. Determine the energy dissipated in fracturing the post specimen. The work ΔU done by force F_X on the pendulum mass during movement d_X is equal to the change in kinetic energy ΔT of the mass; this is also the fracture energy of the post specimen:

$$\Delta U = \Delta T \tag{4}$$

$$\int_0^x F_x dx = \frac{1}{2} m(v_f^2 - v_o^2)$$

Example: Initial and final velocities are 30.3 and 8.5 fps respectively. Then the change in kinetic energy (fracture energy) is

$$\Delta T = \frac{1}{2} m(v_f^2 - v_o^2) = \frac{4{,}000}{2(32.2)}\left[(8.5)^2 - (30.3)^2\right] = 52{,}500 \text{ ft-lb}$$

5. Calculate post displacement during impact. Assume mass velocity changes linearly with time; thus

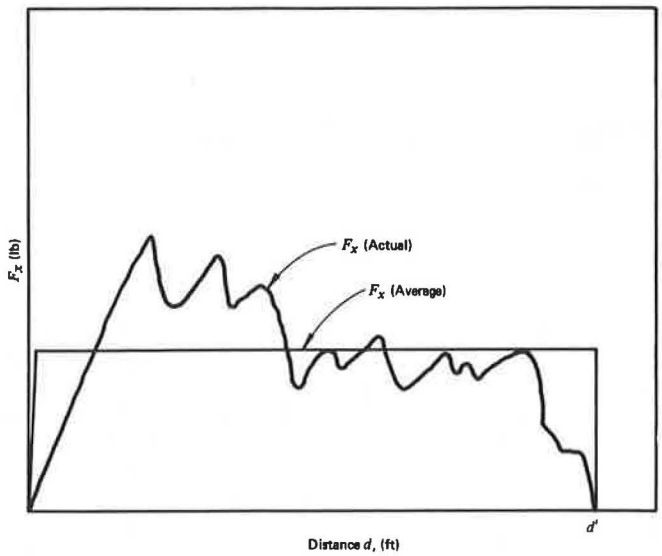

Figure 13. Relationship between actual and average force.

$$d' = \left(\frac{v_f + v_o}{2}\right)(t_f - t_o) \tag{5}$$

where v_f, v_o, t_f, and t_o are respectively final and initial velocities and final and initial time.

Example: Let v_f and v_o be 30.3 and 8.5 fps and t_f and t_o be 200 and 0 msec; then

$$d = \left(\frac{8.5 + 30.3}{2}\right)(200 - 0) = 3.88 \text{ ft}$$

6. Calculate the average force during specimen displacement

$$\int_0^x F_x dx = \overline{F}_x d' = \Delta U \tag{6}$$

where $\overline{F}_x$ is an idealized constant force that acts through distance d′ (Fig. 13).

Example: Let ΔU be 52,500 ft-lb and d′ be 3.88 ft; then

$$\overline{F}_x = \left(\frac{U}{d'}\right) = \left(\frac{52,500}{3.88}\right) = 13,520 \text{ lb}$$